

Document downloaded from:

<http://hdl.handle.net/10251/43474>

This paper must be cited as:

Gómez Lozano, V.; Uris Martínez, A.; Candelas Valiente, P.; Belmar Ibáñez, F. (2013). Acoustic transmission through perforated plates with fractal subwavelength apertures. *Solid State Communications*. 165:11-14. doi:10.1016/j.ssc.2013.04.012.



The final publication is available at

<http://dx.doi.org/10.1016/j.ssc.2013.04.012>

Copyright Elsevier

# ACOUSTIC TRANSMISSION THROUGH PERFORATED PLATES WITH FRACTAL SUBWAVELENGTH APERTURES

Vicente Gómez-Lozano, Antonio Uris<sup>\*</sup>, Pilar Candelas, Francisco Belmar

Centro de Tecnologías Físicas, Unidad Asociada ICMM-CSIC/UPV, Universitat

Politécnica de Valencia, Av. Naranjos s/n. 46022 Valencia, Spain

\*Corresponding author: [auris@fis.upv.es](mailto:auris@fis.upv.es)

## ABSTRACT

The acoustic transmission response of plates perforated with fractal subwavelength holes array is studied. The Sierpinski Carpet pattern is used as fractal geometry. Ultrasound transmission spectra show that each iterative Sierpinski Carpet has the characteristic peaks and dips of the lattice constant of each array that formed the pattern. The angular dependency of the transmission coefficients shows a complex interplay between Fabry-Perot resonances, Wood anomaly minima and Lamb modes.

*Keywords:* Subwavelength, fractal pattern, Sierpinski carpet, perforated plate.

## 1. Introduction

In the last years, research into extraordinary optical transmission [1] through metallic films perforated with subwavelength apertures arrays has been extrapolated to acoustics. This new area of study has attracted much attention throughout the last five years for clarifying the basic physics of the phenomenon as well as to develop devices

for engineering applications. Zhou and Kriegsman [2] predicted the complete sound transmission through two-dimensional subwavelength hole-arrays by means of the scattering matrix technique for the first mode of the cavity. The experimental confirmation of complete acoustic transmission was reported for a perforated brass plate immersed in water by Hou et al. [3] and for a slit array made of steel in air by Lu et al. [4]. Fabry-Perot resonances in the hole produce the main contribution to the full transmission peaks. It has been argued [3] that the existence of a full transmission peak near to the Wood anomaly [5] is due to an array resonance. The dispersion relation of leaky and bounded surface modes was derived in the hard-solid limit for one- and two-dimensional arrays of square holes by Christensen et al. [6] and it was pointed out the hybridization of these modes with the Fabry-Perot resonances. Estrada et al. [7] showed that perforated aluminium plates immersed in water at ultrasonic frequencies exhibit extraordinary sound attenuation well beyond that predicted by the mass law equation due to Wood anomalies. Estrada et al. [8, 9] also showed that, the position and the width of the transmission peak can be tuned changing geometrical parameters like the filling fraction of holes and the lattice geometry of perforated plates.

So far, the investigations on acoustic transmission through subwavelength apertures are restricted to plates with periodic arrays of apertures. Hao et al. [10] studied the acoustic transmission through plates perforated with a quasiperiodic array of subwavelength apertures. The results showed strong resonant transmissions, attributed to the coherent diffraction by the long-range order of the quasiperiodic structure. Hao et al. [11] also studied the acoustic transmission through plates with quasiperiodic surface corrugations. The results showed that the resonant transmissions observed in the subwavelength region can be attributed to the collective excitation of the antisymmetric

Stoneley surface modes. Fractal geometries [12] are examples of aperiodic structures and possess self-similar properties.

With the purpose of identifying how the geometry self-similarity influences the acoustic transmission, in this letter we consider water-immersed brass plates perforated with fractal-featured aperture array in a Sierpinski Carpet pattern. The acoustic transmission and the physical origins are analyzed and discussed.

## **2. Experimental setup**

Underwater ultrasound has been chosen to measure the acoustic transmission through perforated plates. The geometrical parameters to describe perforated plates are the diameter of the hole  $d$ , the array periodicity  $a$  and the plate thickness  $h$ . The experimental setup is based on the well known ultrasonic immersion transmission technique. This technique makes use of a couple of transmitter/receiver ultrasonic transducers (see Figure 1). Two different couples of transducers were used: one couple with a center frequency of 250 kHz and a frequency range between 155-350 kHz and the other couple with center frequency of 500 kHz and a frequency range between 350-650 kHz. Each transducer was located at a distance larger than that of its nearfield distance (43 mm) from the plate and aligned with respect to the plate. A pulse is launched by the emitter piston transducer through the inspected plate. Then, the signal is detected by the receiving piston transducer and acquired by the pulser/receiver, post amplified and digitized by a digital PC oscilloscope (Picoscope model 3224). Time domain data is finally analyzed after averaging 100 different measures. Time window is set to be wide enough to collect only direct transmission through the plate and to avoid indirect transmission due to lateral reflections [13]. The transmission spectrum is then calculated

as  $\frac{|T/\omega|^2}{|H_0/\omega|^2} = \frac{|H/\omega|^2}{|H_0/\omega|^2}$  from the power spectrum of the signal  $H(\omega)$  normalized

with the reference signal power spectrum  $H_0(\omega)$  measured without the sample plate.

Typically, angle dependent measurements were done in angle steps of  $\Delta\chi = 1^\circ$  and comprising  $0^\circ \leq \chi \leq 60^\circ$ .

The measurements were made using brass plates with 350 mm in width and 450 mm in length ( $\rho = 7890 \text{ kg/m}^3$ ,  $c_l = 5670 \text{ m/s}$ ,  $c_t = 3230 \text{ m/s}$ ) and 2 mm thickness, immersed in water ( $\rho = 1000 \text{ kg/m}^3$ ,  $c_l = 1480 \text{ m/s}$ ).

Three iterative generations of the Sierpinski Carpet pattern were used. In the first step, a periodically square distribution of circular holes having diameter 1 mm and a unit cell period of 3 mm, drilled on the brass plate was used (see Figure 2a). The second iterative generation was made with a square distribution of circular holes having diameters 1 mm and 3 mm and a unit cell period of 9 mm (see Figure 2b). The last generation was made with a square distribution of circular holes having diameters 1 mm, 3 mm and 9 mm and a unit cell period of 27 mm (see Figure 2c).

### 3. Results and discussion

We can explore the transmission properties of the Sierpinski Carpet pattern by calculating and measuring transmitted sound power coefficient,  $\tau$ , as a function of the frequency,  $f$ , in the fluid at normal incidence. The transmission sound power was calculated by solving the sound wave equation within a hard-solid model and reported in [14, 15]. Figure 3 shows a comparison between measured and calculated transmission spectra at normal incidence for each of the three iterations Sierpinski Carpet patterns samples considered. The measurements are in good agreement with the calculated results even though there are some differences between them. The measured

transmission peaks are broader than the calculated ones due to dissipative losses that have not been taken into account in the calculation model and due to experimental errors [8]. The slightly change in the frequencies of the characteristics peaks that were not predicted by the calculated results is due to the calculations were carried with a rigid-solid model and the elastic movement of the plate coupled with the surrounding fluid had not been considered. The transmission spectra for the periodically square distribution of circular holes having diameter 1 mm and a unit cell period of 3 mm are depicted in Figure 3(a). The transmission peaks observed at the frequencies  $\sim 280$  and  $\sim 480$  kHz correspond to the Fabry-Perot resonances. The minimum transmission at the frequency  $\sim 490$  kHz (corresponding to the wavelength 3 mm) results from the Wood anomaly. The transmission spectra of the second iterative generation, made with circular holes having diameters 1 mm and 3 mm and a unit cell period of 9 mm, are showed in Figure 3(b). It appears moreover a full transmission peak at the frequency  $\sim 160$  kHz and transmission dips at the frequencies  $\sim 170$  and  $\sim 220$  kHz corresponding to the Wood anomaly of the array of lattice period 9 mm. The third iteration, made with holes having diameters 1 mm, 3 mm and 9 mm and a unit cell period of 27 mm, is depicted in Figure 3(c). The transmission spectra are similar to the second iteration due to the lattice resonances of period 27 mm is around 50 kHz, out of our frequency range. Both calculated and measured results make it clear that the normal incidence transmission curve of each iterative generation of the Sierpinski Carpet structure has the characteristics peaks and dips each contributed array.

The experimental transmitted sound power  $\vartheta$  as a function of the parallel wavevector  $k_x \cdot a/\phi$  in the BX direction and the normalized frequency  $\omega a/2\phi c$  is observed from figure 4. Again first (figure 4(a)-(a')), second (Figure 4(b)-(b')) and third iterative generation (Figure 4(c)-(c')) are studied. Plots on the right are the same than those on

the left with the inclusion, for reference, of Wood anomaly curves of each unit cell period.

Complex interaction between minima and maxima is present in the spectra and it makes clear that the symmetry of the array results in a high angular dependence of the spectra. The measurement in the periodically square distribution of circular holes having diameter 1 mm and a unit cell period of 3 mm (Figure 4(a)) shows the  $S_0$  Lamb mode (denoted by the arrow) interacting with the lattice resonances at  $k \cdot a/\phi \sim 0.5$  and 1. In agreement with the normal incidence results from Fig. 3(a), the first order Fabry-Perot full transmission peak at the frequency  $\sim 280$  kHz can be observed when  $\omega a/2\phi c \sim 0.55$ . The peak at the frequency  $\sim 480$  kHz is placed at  $\omega a/2\phi c \sim 1$ , immediately below the Wood anomaly minimum that is evident when the incidence angle is varied. Due to the peak is quite narrow and to the limitations of the measurement system, it cannot be clearly observed. Figure 4(a') is the same than Figure 4(a) with the inclusion of Wood anomalies curves. The second iterative generation, made with circular holes having diameters 1 mm and 3 mm and a unit cell period of 9 mm, is shown in Figures 4(b)-(b'). The Fabry-Perot full transmission peak at the frequency  $\sim 280$  kHz can be clearly observed when  $\omega a/2\phi c \sim 1.7$ , but the transmission peaks at 160 and 480 kHz corresponding to  $\omega a/2\phi c \sim 1$  and  $\sim 1.33$ , respectively, are not clearly observed because they are overshadowed by the overall transmission. The transmissions dips at the frequencies  $\sim 170$  and  $\sim 220$  kHz corresponding to the Wood anomaly of the array of lattice period 9 mm are observed at  $\omega a/2\phi c \sim 1.01$  and 1.34. The Wood anomaly minima of the 3 mm lattice period array observed at  $\omega a/2\phi c \sim 3$ . It is also observed a complex the interplay between Wood minima, resonance interference and transmission peaks also found in [15]. These features remain in the third iteration made with holes having

diameters 1 mm, 3 mm and 9 mm and a unit cell period of 27 mm, as Figures 4(c)-(c') show, due to the lattice resonances of period 27 mm is out of the transducers frequency detection range.

#### **4. Conclusions**

Sound transmission through perforated plates with Sierpinski Carpet pattern has been studied. The experimental results agree with the calculated ones. The results show that each iterative generation of the Sierpinski Carpet structure has the characteristics peaks and dips of each contributed array, so it is possible to achieve transmission peaks and dips at different frequencies simultaneously with the same sample. Prospective applications, such as ultrasonic filters, can be anticipated.

#### *Acknowledgments*

This work has been supported by the Spanish MICINN (MAT2010-16879) and Universitat Politecnica de Valencia (PAID-06-10-1839).

#### **References**

- [1] T.W. Ebbesen, H. J. Lezec, H. F. Ghaemi, T. Thio and P.A. Wolf, Nature (London) 391 (1998) 667-669.
- [2] L. Zhou and G. A. Kriegsmann, J. Acoust. Soc. Am. 121 (2007), 3288-3299.
- [3] B. Hou, J. Mei, M. Ke, W. Wen, Z. Liu, J. Shi and P. Sheng, Phys. Rev. B 76 (2007), 054303-054309
- [4] M. Lu, X. Liu, L. Feng, J. Li, C. Huang, Y. Chen, Y. Zhu, S. Zhu and N. Ming, Phys. Rev. Lett. 99 (2007), 174301-174301.

- [5] R. W. Wood, *Phil. Mag.* 4 (1902), 396-402.
- [6] J. Christensen, L. Martin-Moreno, F.J. Garcia-Vidal, *Phys. Rev. Lett.* 101, 014301, (2008) .
- [7] H. Estrada, P. Candelas, A. Uris, F. Belmar, F. J. Garcia de Abajo, F. Meseguer, *Phys. Rev. Lett.* 101 (8) (2008) 084302-084305.
- [8] H. Estrada, P. Candelas, A. Uris, F. Belmar, F. Meseguer, F. J. Garcia de Abajo, *Appl. Phys.Lett.* 93 (1) (2008) 011907-011909.
- [9] H. Estrada, P. Candelas, A. Uris, F. Belmar, F. J. Garcia de Abajo, F. Meseguer, *Appl. Phys. Lett.* 95 (5) (2009) 051906-051906.
- [10] R. Hao, H. Jia, Y. Ye, F. Liu, C. Qiu, M. Ke, Z. Liu, *Eur. Phys. Lett.* 92 (2010) 24006.
- [11] R. Hao, C. Qiu, Y. Hu, K. Tang, Z. Liu, *Physics Letters A* 375 (2011) 4081-4084.
- [12] B. B. Mandelbrot, *The Fractal Geometry of Nature* (W.H. Freeman & Co., New York) 1983.
- [13] D. E. Chimenti, D. Fei, *Int. J. Solid Struct.* 39 (2002) 5495-5513
- [14] H. Estrada, P. Candelas, A. Uris, F. Belmar, F. Meseguer, F. J. García de Abajo, *Wave Motion* 48 (2011) 235–242
- [15] H. Estrada, V. Gomez-Lozano, A. Uris, P. Candelas, F. Belmar, F. Meseguer, *J.Phys.: Condens. Matter* 23 (2011) 135401

## FIGURES CAPTIONS

Figure 1. (a) Diagram of the experimental setup. This setup makes possible to explore the transmission coefficient at different angles of incidence.  $Q_0$  corresponds to the component of the incident wavevector  $k_0$  which is parallel to the plate. The inset shows a diagram of the geometrical parameters of the perforated plate where  $d$  is the hole diameter,  $a$  the array periodicity and  $h$  the plate thickness.

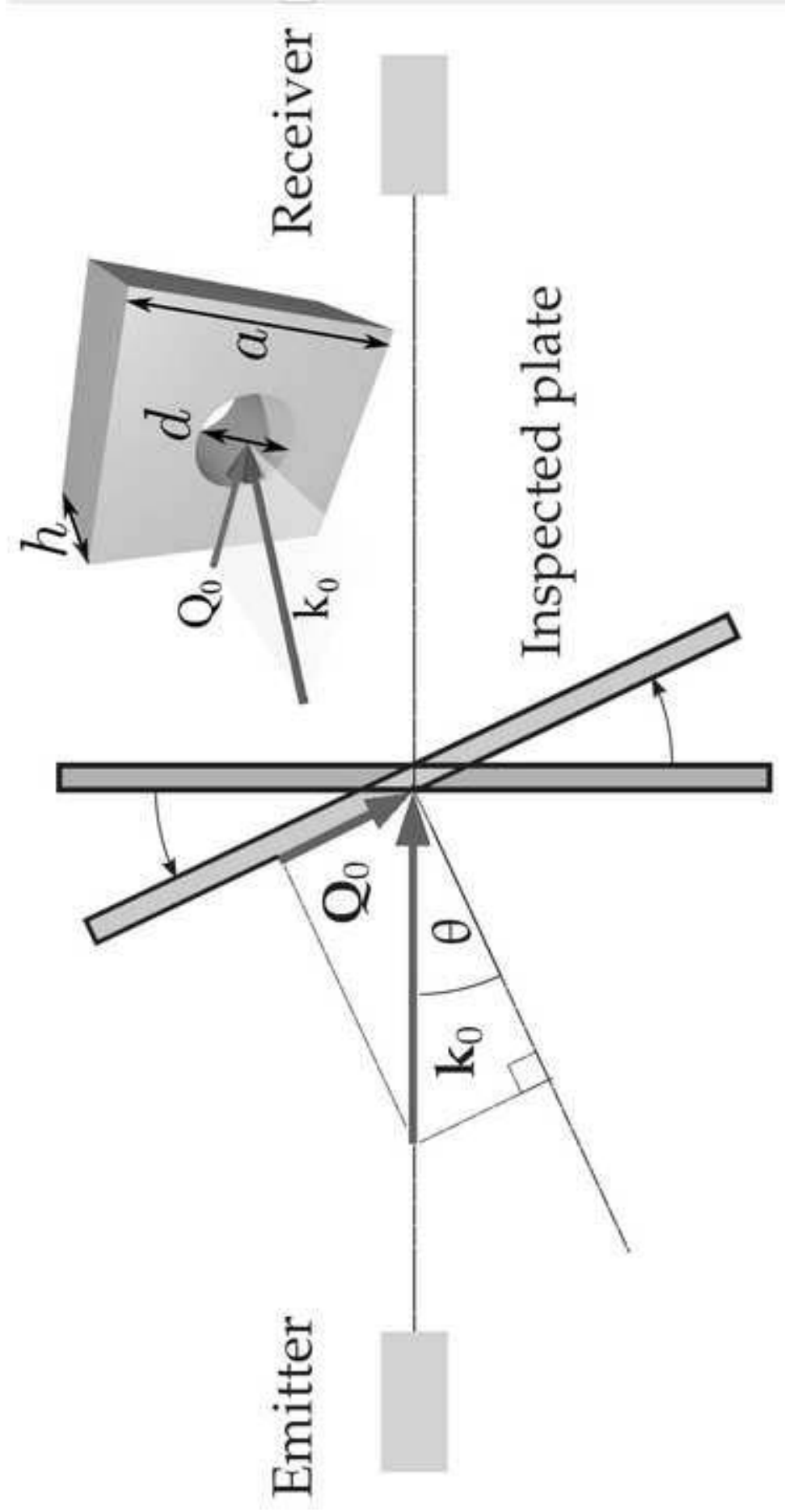
Figure 2. Schematic diagram of the iterative generations of the Sierpinski Carpet pattern. (a) First iteration with circular holes of diameter 1 mm and unit cell period 3 mm. (b) Second one with circular holes of diameters 1 mm and 3 mm and unit cell period 9 mm. (c) Third iterative generation with circular holes of diameters 1 mm, 3 mm and 9 mm and unit cell period 27 mm.

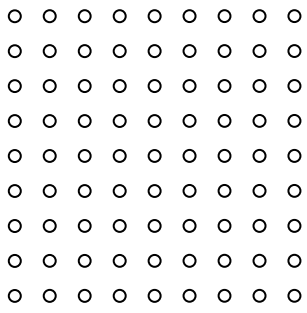
Figure 3. Measured (solid curve) and calculated (dashed curves) transmitted sound power coefficient at normal incidence as a function of the frequency for the three iterative generations of the Sierpinski Carpet pattern. (a) First iteration with circular holes of diameter 1 mm and unit cell period of 3 mm. (b) Second one with circular holes of diameters 1 mm and 3 mm and unit cell period of 9 mm. (c) Third iterative generation with circular holes of diameters 1 mm, 3 mm and 9 mm and unit cell period of 27 mm.

Figure 4. Measured transmitted sound as a function of the parallel wavevector  $k_{\parallel} \cdot a / \phi$  in the BX direction and the normalized frequency  $\omega a / 2\phi c$ . The transmitted sound is represented in dB scale. (a) First iteration with circular holes of diameter 1 mm and unit

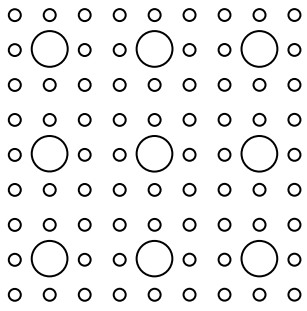
cell period,  $a = 3$  mm. In (a') Wood anomaly minima are added to the plot (white solid lines). (b) Second one with circular holes of diameters 1 mm and 3 mm and unit cell period,  $a = 9$  mm. In (b') Wood anomaly minima are added to the plot for unit cell period,  $a = 3$  mm (white solid lines) and for unit cell period,  $a = 9$  mm (black solid lines). (c) Third iterative generation with circular holes of diameters 1 mm, 3 mm and 9 mm and unit cell period  $a = 27$  mm. In (c') Wood anomaly minima are added to the plot for unit cell period,  $a = 3$  mm (white solid lines) and for unit cell period,  $a = 9$  mm (black solid lines). Wood anomaly minima for unit cell period  $a = 27$  mm is out of the transducers frequency detection range.

Figure 1- B&W  
[Click here to download high resolution image](#)

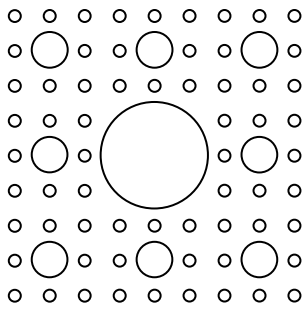




(a)



(b)



(c)

FIGURE 2

Figure 3- B&W  
[Click here to download high resolution image](#)

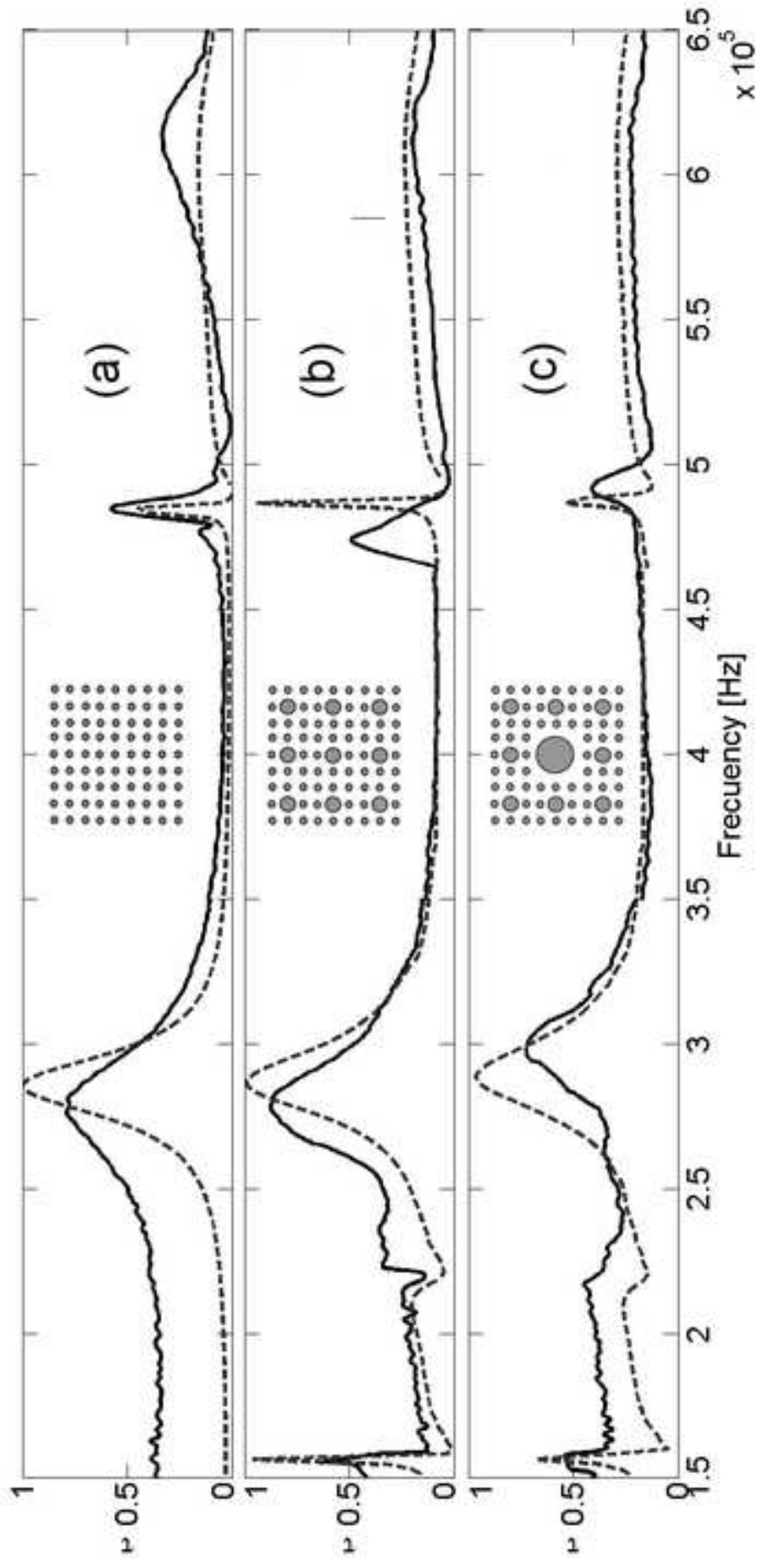


Figure 4- B&W  
[Click here to download high resolution image](#)

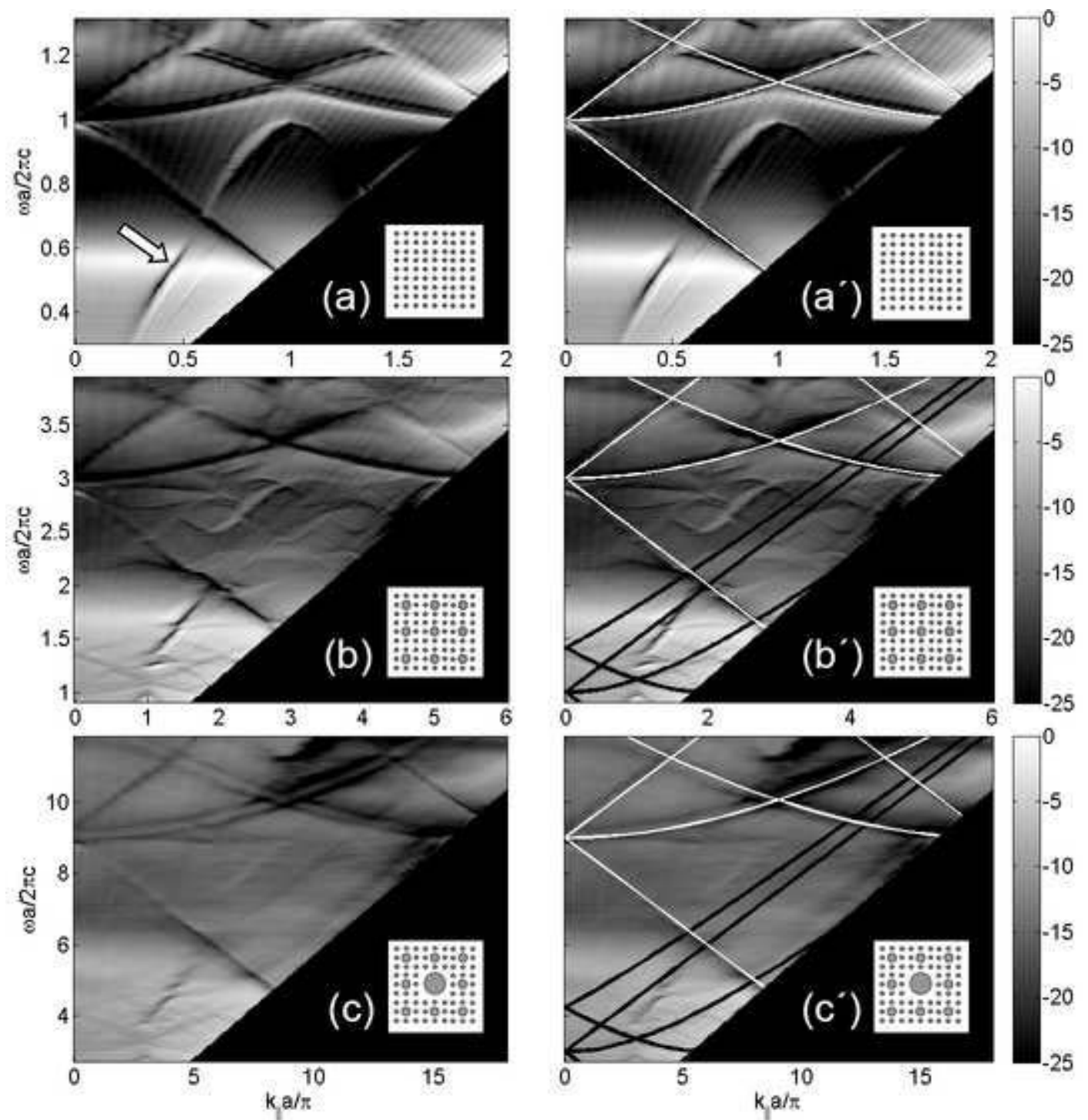


Figure 1 - Colour  
[Click here to download high resolution image](#)

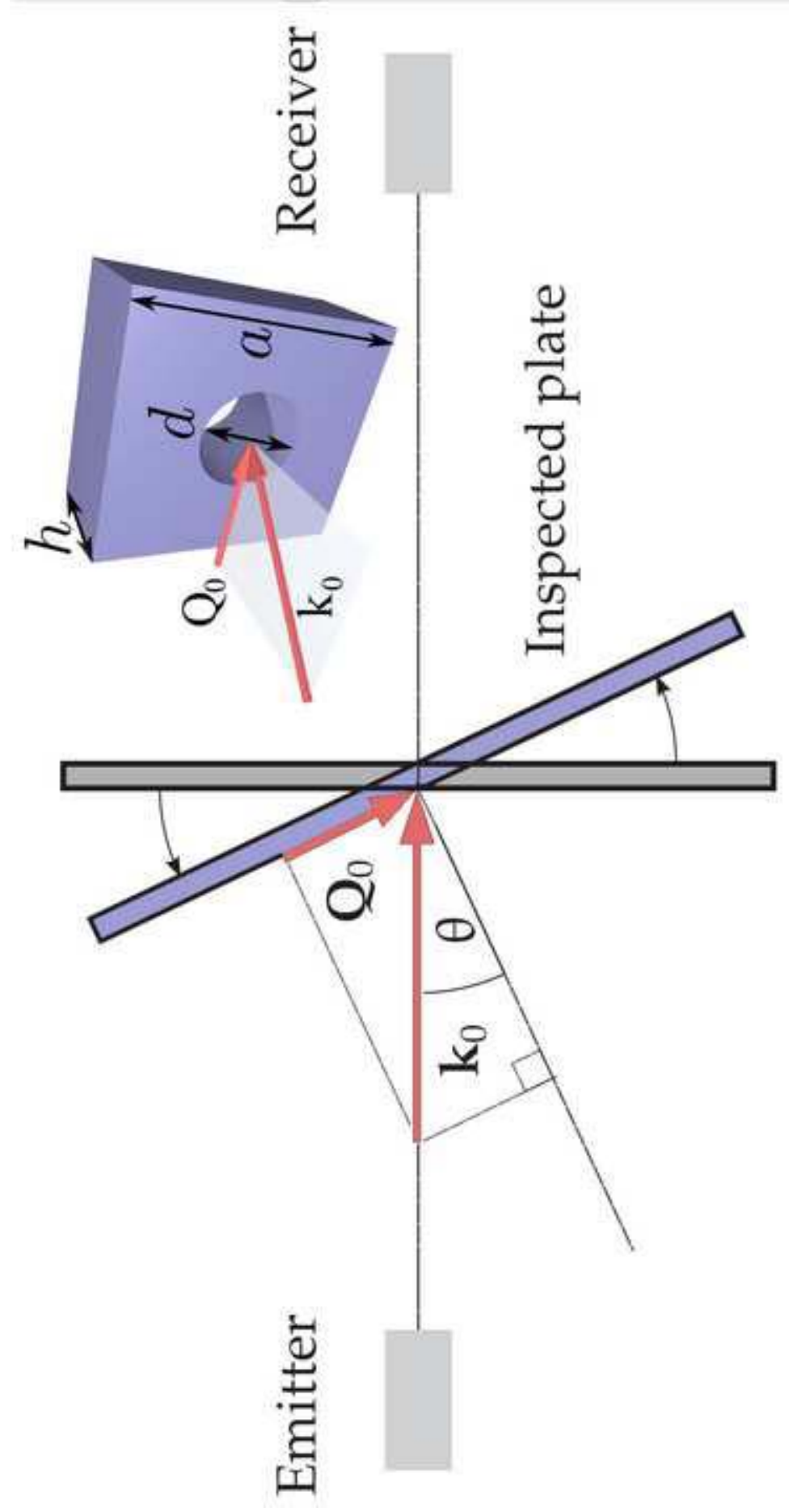


Figure 3- Colour  
[Click here to download high resolution image](#)

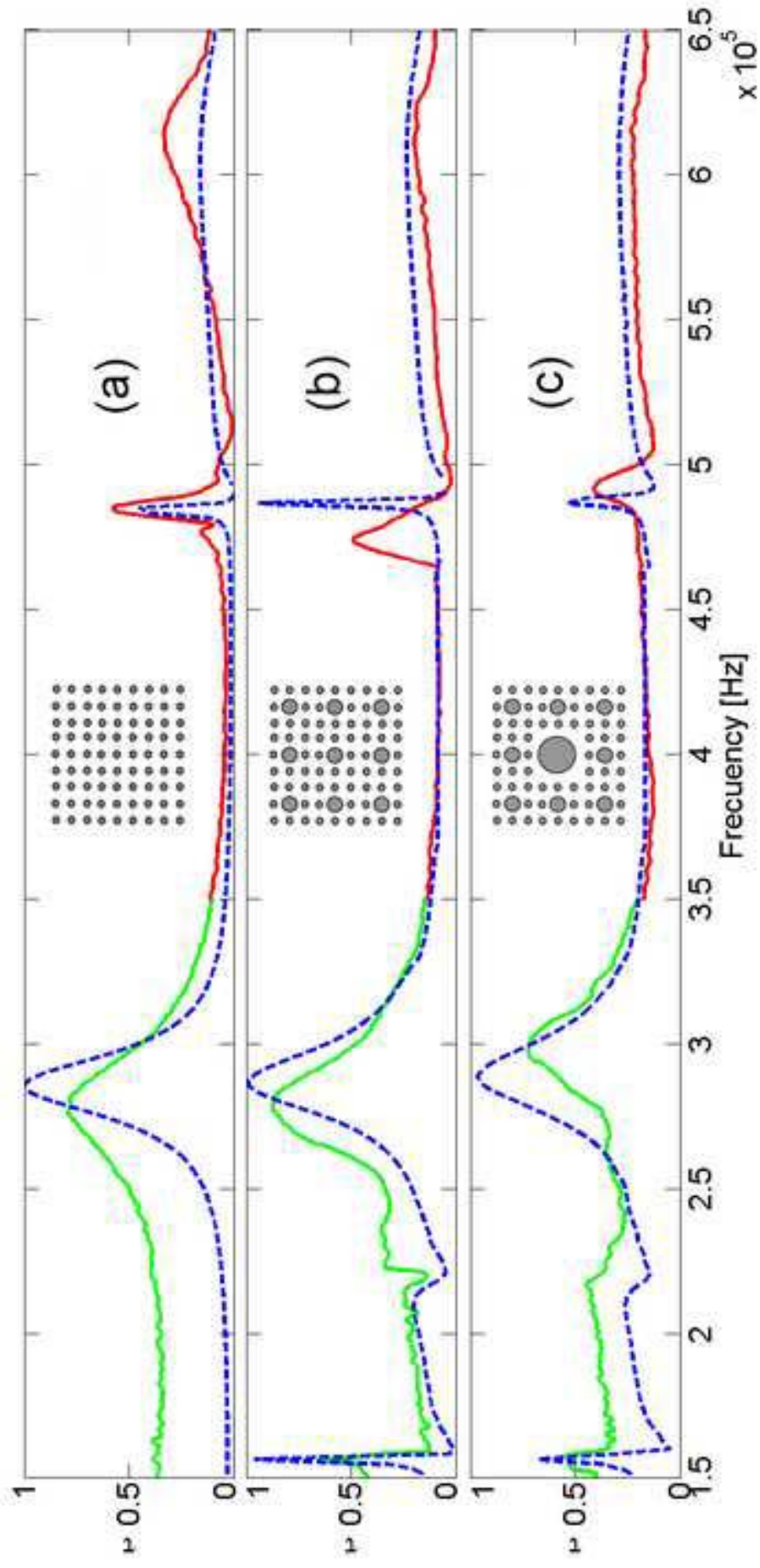


Figure 4- Colour  
[Click here to download high resolution image](#)

